Available online at www.sciencedirect.com
ScienceDirect
Aerosol Science 39 (2008) 759–769
Journal of Aerosol Science
www.elsevier.com/locate/jaerosci

Performance characteristics of the ultra high sensitivity aerosol spectrometer for particles between 55 and 800 nm: Laboratory and field studies

Yong Cai*, Derek C. Montague, Wiesje Mooiweer-Bryan, Terry Deshler

Department of Atmospheric Science, University of Wyoming, Laramie, WY 82071, USA

Received 15 January 2008; received in revised form 15 April 2008; accepted 15 April 2008

Abstract

A new optical particle counter, the Particle Metrics, Inc., ultra high sensitive aerosol spectrometer (UHSAS), has been used to size aerosol particles both in our laboratory, and at a remote mountain-top site in Wyoming. The laboratory studies show that the UHSAS measured diameters of polystyrene latex (PSL), ammonium sulfate, and ammonium nitrate particles are within 10% of those determined by a scanning mobility particle sizer (SMPS), as are those for non-spherical sodium chloride particles and PSL doublets. The UHSAS detection efficiency is close to 100% for particles larger than 100 nm and concentrations below 3000 cm^{-3}, but decreases both for smaller particles and for higher concentrations considerably. The field measurements confirm these observations and also demonstrate good agreement of particle concentration measurements between the UHSAS, SMPS, and a passive cavity aerosol spectrometer probe (PCASP) in the same size ranges.

Keywords: UHSAS; Size distribution; Irregular particle; OPC; Ambient aerosol

1. Introduction

Investigation of the effects of atmospheric aerosols on global climate and human health relies on accurate measurements of aerosol concentration and size distribution. Light scattering provides an extremely sensitive tool for the determination of aerosol concentration and size (McMurry, 2000). Consequently, optical particle counters (OPCs) have been used extensively in atmospheric aerosol research, air pollution studies, and indoor air quality monitoring. OPCs are widely used in aerosol measurements not only because they provide *in situ* measurements for continuous monitoring, but also because they are compact, robust, and require minimal maintenance. However, in most applications, the OPCs being used have in general had relatively large lower size detection limits and a small number of size bins (Weschler & Shields, 2003). The low size resolution and restricted size range can be problematic for some applications. In addition, OPCs operating at visible wavelengths often suffer from a non-monotonic counter response in the so-called "Mie resonant" region of light scattering (Barnard & Harrison, 1988).

To improve size resolution and the detection of small particles, Particle Metrics, Inc. (Boulder, Colorado) developed an ultra high sensitivity aerosol spectrometer (UHSAS). It is designed to size particles accurately and precisely in the

* Corresponding author. Tel.: +1 307 766 3273; fax: +1 307 766 2635.
E-mail address: ycai@uwyo.edu (Y. Cai).

0021-8502/$ - see front matter © 2008 Elsevier Ltd. All rights reserved.
doi:10.1016/j.jaerosci.2008.04.007

range from ∼ 55 to ∼ 1000 nm diameter. The spectrometer classifies particles in 99 size channels within its detection range. This study represents one of the first independent comprehensive investigations of the performance of the UHSAS under both controlled laboratory conditions and at a field site. For the laboratory experiments, particle concentrations are compared to those measured by a condensation particle counter (CPC) while particle sizes are compared to those determined with a scanning mobility particle sizer (SMPS). Field measurements covered two weeks during summer 2006 at our remote mountain-top observatory at Elk Mountain, Wyoming (EMO; N41°38′, W106°32′), a site that is minimally impacted by anthropogenic aerosol sources. Particle concentrations and size distributions for the ambient aerosol were examined and compared using the UHSAS, CPC, SMPS, and PCASP (passive cavity aerosol spectrometer probe).

2. Characterization of the UHSAS

The UHSAS is an optical-scattering laser-based aerosol spectrometer. A semiconductor-diode-pumped Nd^{3+}:YLF solid-state laser, operating at 1.054 μm with an intracavity power of ∼ 1 kW, is employed to illuminate the particles. Its detection system consists of two pairs of Mangin mirrors capable of collecting light over a large solid angle (22°–158°). The sheath flow is internally set at 910 cm^3 / min and sample flow can be adjusted from 13 to 130 cm^3 / min. The design of the scattering optics and the high intensity of the illuminating laser permit the detection of particles down to 55 nm diameter. As the laser wavelength is 1.054 μm, the theoretical response of the UHSAS over the size range covered increases monotonically and approximately linearly with increasing particle size at different refractive indices, as shown on the log–log plot in Fig. 1. The approximately linear response range in log space is much broader than that previously achieved by visible wavelength OPCs (Ames, Hand, Kreidenweis, Day, & Malm, 2000). All of the particle sizes measured by the UHSAS in the laboratory fell in this range. Therefore, the obtained UHSAS optical sizes can be readily corrected for different refractive indices, as necessary, following the method proposed by Ames et al. (2000).

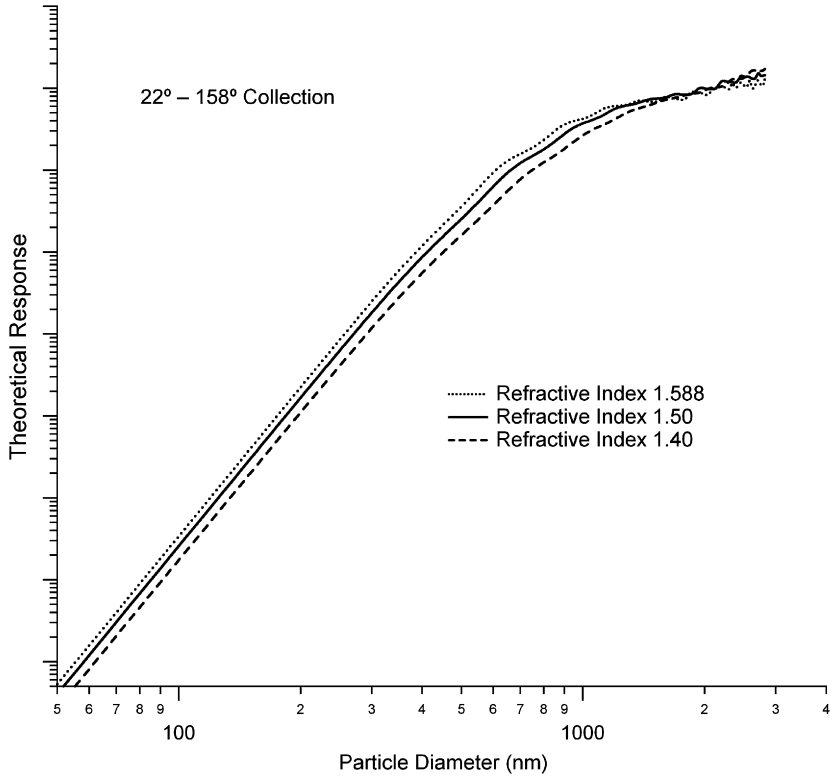

Fig. 1. Theoretical response of the UHSAS at different refractive indices for illumination of the scattering region by a 1054 nm laser and a collection angle of 22°–158° from the forward direction.

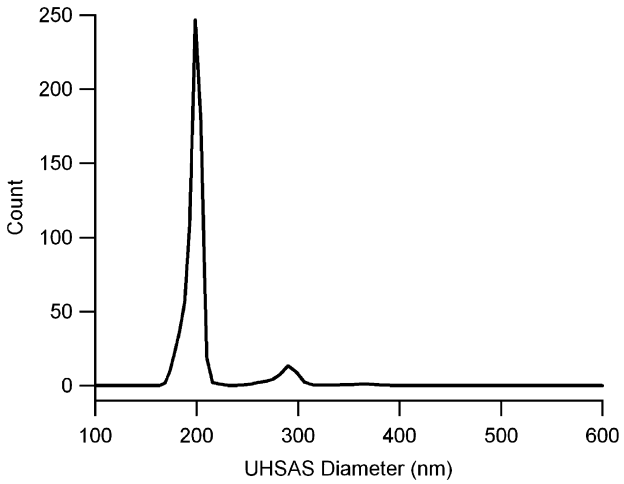

Fig. 2. Size distribution of 199 ± 6 nm PSL particles and their aggregates measured by the UHSAS.

Table 1
PSL spherical particle diameter and the measured SMPS and UHSAS diameters

PSL diameter (nm)	91	125	**152**	176	**199**	**269**	343	**491**	653
SMPS diameter (nm)	91	126	**154**	173	**202**	**269**	344	**496**	661
UHSAS diameter (nm)	83	120	**152**	169	**199**	**268**	341	**495**	670

Particles with **bold diameters** were used for calibration.

2.1. Laboratory experimental procedure

All of the aerosol particles were generated by an atomizer (TSI Model 3076) and dried with a diffusion dryer (TSI Model 3062). A classifier (TSI, Model 3081 LDMA) was used to select monodisperse particles. After being re-neutralized with a polonium charger and diluted by clean dry air, the monodispersed particles were measured simultaneously by a UHSAS, a TSI Model 3010 butanol-based CPC, and a SMPS (TSI Model 3936L10) equipped with a second TSI Model 3010 CPC. Vaisala sensors (HMP238) were used to measure the relative humidity (RH) of the sample flow both upstream of the classifier and downstream of the aerosol dilution chamber.

2.2. Size characterization

Accurate particle sizing across the full dynamic range of the UHSAS is achieved by concatenating the four separate gain stages of the instrument during the calibration process. The relative gains of each stage are determined through measurements on particles that have a broad size distribution such as ambient particles. The relative coefficients between gain stages are then set to provide a smoothed size distribution. Absolute calibration to relate specific gain values to particle diameter, is achieved using polystyrene latex (PSL) particles (Duke Scientific) with diameters 152, 199, 269, and 491 nm, to cover the gain stage size ranges. Instrumental responses (millivolts) from these PSL particles are used to define the absolute calibration curve, which remains the manufacturer's calibration for 100 nm particles. After calibration, the instrument was checked using five additional PSL particle sizes. Fig. 2 shows the response of the UHSAS to 199 ± 6 nm PSL particles. The first, large peak results from 199 nm spherical PSL particles, while the second, small peak indicates the presence of PSL aggregates. During the UHSAS calibration, PSL particle size was also independently assessed and confirmed by the SMPS. Table 1 shows the measured results. Although large diameter differences measured by the UHSAS and SMPS were observed for some individual PSL sizes, the linear regression for all PSL sizes shows less than 1% difference on average.

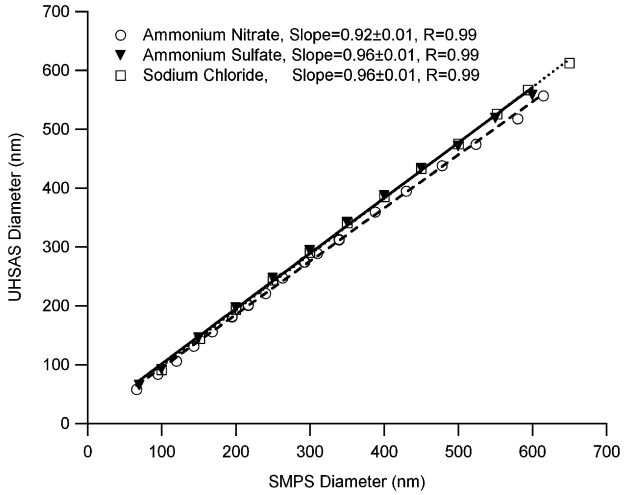

Fig. 3. Comparison of the UHSAS and SMPS measured sizes for ammonium nitrate, ammonium sulfate, and sodium chloride particles.

UHSAS performance was also tested using ammonium sulfate, ammonium nitrate, and sodium chloride particles. Particles classified by the DMA were mixed with dry, clean air and the sample RH was adjusted to below 15%. To reduce evaporative loss of ammonium nitrate, the lengths of conductive tubing connecting the experimental instruments were minimized, and all tubing was preconditioned with dried ammonium nitrate aerosol prior to the commencement of measurements (Zelenyuk, Cai, Chieffo, & Imre, 2005). Those between the dilution chamber output and the inlets of the SMPS and UHSAS were the same length to equalize potential losses. Fig. 3 shows a scatter plot comparison of the results. Within the size range from 100 to 650 nm, the UHSAS measured sizes are very similar to those from the SMPS, for all three salts. Larger differences in the measured sizes are observed for smaller particles. The regression lines shown in Fig. 3 are fitted only to particle diameters > 70 nm, and are constrained to pass through the plot origin. For ammonium sulfate particles, the measured UHSAS size was consistently $4 \pm 1\%$ smaller than the SMPS size, while for ammonium nitrate particles, the measured UHSAS sizes were $8 \pm 1\%$ smaller than those from the SMPS. At higher humidity, water retention by the particles might well affect sizing, but it is unlikely to be important here, where the RH of the sample stream in the laboratory was $< 15\%$, well below the ammonium sulfate efflorescence RH (37%) reported by Tang and Munkelwitz (1994). Although ammonium nitrate particles exhibit no distinct efflorescence point (Lightstone, Onasch, Imre, & Oatis, 2000), only minor amounts of residual water would have been retained by these particles at the low RH of the sample stream both in the laboratory experiments and in those conducted at Elk Mountain. In addition, within experimental error, the measured SMPS sizes were the same as the classified sizes for ammonium sulfate particles, and 1.2% lower on average than the classified sizes for ammonium nitrate particles, confirming that there was little, if any, water evaporation from the particles during the dilution and drying process, suggesting that the particles were essentially dry.

Perry, Hunt, and Huffman (1978) and Liu, Leaitch, Strapp, and Wasey (1992) reported lower scattering intensities for cubic particles than for spherical particles with the same volumetric diameter and refractive index; so these cubic particles tend to be under-sized by OPCs. Contrastingly, the measured mobility size of particles tends to increase as they become more irregularly shaped (DeCarlo, Slowik, Worsnop, Davidovits, & Jimenez, 2004). Non-spherical cubic particles might therefore be expected to display a difference between their measured mobility and optical sizes, a presupposition not supported by our measurements, which show good agreement between the SMPS and UHSAS sizes for sodium chloride particles. The regression line for sodium chloride, shown in Fig. 3, is coincident with that for ammonium sulfate, and therefore has the same slope (0.96 ± 0.01).

PSL aggregates, generated using aqueous suspensions of high concentrations of monodisperse PSL particles (diameter 125 and 199 nm), were simultaneously sized by the SMPS and UHSAS, with the results shown in Table 2. For the two PSL doublets, the diameters measured by the UHSAS and SMPS are in reasonably good agreement. For the PSL triplets, however, the UHSAS measured sizes are about 10% smaller than those measured by the SMPS. The results suggest that for PSL triplets, shape irregularities cause a large difference between the optical and mobility

Table 2
Measured SMPS and UHSAS diameters for PSL spheres and aggregates

PSL diameter (nm)	No. of PSL sphere	SMPS (nm)	UHSAS (nm)	Volumetric equivalent diameter d_{ve} (nm)
125	1	126	120	125
	2	168	162	158
	3	202	186	181
199	1	202	199	199
	2	265	262	251
	3	311	292	287

diameters, whereas for PSL doublets, they have a lesser influence. Furthermore, while the sizes measured by the two instruments are different and both larger than the corresponding volume-equivalent diameters (d_{ve}) of the aggregates, those determined by the UHSAS are in better agreement with the aggregate volume-equivalent diameters. Analogous agreement between optical and volume equivalent diameter was also reported by Pinnick & Rosen (1979) using an ASASP-300, and by Quinten, Friehmelt, & Ebert (2000) using a white light OPC. Our results suggest that the measured size differences between the two instruments for PSL aggregates result primarily from the shape-based increase of particle mobility size by the SMPS.

In summary, for spherical PSL particles, the measured UHSAS and SMPS sizes agree within 1% after a careful calibration of the instruments. For irregular particles such as ammonium sulfate, sodium chloride, and PSL doublets, the UHSAS and SMPS sizes differ by less than 5%. For PSL triplets, the measured size difference between the SMPS and UHSAS is larger, but still $< 10\%$. Additionally, for PSL aggregates, the UHSAS measured sizes approximate the particle volume-equivalent diameter better than those from the SMPS. Therefore, the influence of particle shape on UHSAS measured particle size can be disregarded to a first approximation. Aged ambient submicrometer particles are expected to most likely have a similar or lower irregularity (Dick, Ziemann, Huang, & McMurry, 1998; Hand et al., 2002); so we do not anticipate that UHSAS measurements of the size of these ambient particles would be significantly in error.

2.3. Concentration comparisons

The dependence of detection efficiency on particle size was investigated by measuring the UHSAS/CPC concentration ratio for small ammonium sulfate particles. The data, shown in Fig. 4, were corrected for multiply charged particles. The ratio rapidly approached unity as the particle diameter increased from 56 to 70 nm. We estimate that for ammonium sulfate, the UHSAS detection efficiency is 50% for particles of diameter 62 ± 2 nm, a threshold value that effectively defines the lower particle size detection limit of the instrument.

Concentration comparisons between the UHSAS and a CPC were carried out in the range 3–5000 cm^{-3}, for all particle types used in the size measurement investigations larger than 100 nm, with the results shown in Fig. 5. For concentrations below 3000 cm^{-3}, UHSAS and CPC measured concentrations are in excellent agreement, with a best fit regression line of slope 0.95 ± 0.01. At higher concentrations larger than 3000 cm^{-3} UHSAS particle number densities declined steadily to 90% of those measured by the CPC as the concentration rose to 4000 cm^{-3}, for particle sizes larger than 100 nm, as shown in Fig. 5. Counting coincidence losses resulting from the $\sim 10\,\mu s$ interaction time and 975 cm^3/ min total flow rate are the main reason for the reduced UHSAS count rates at high particle concentrations. The single outlier in Fig. 5, resulting from a measurement using 62 nm ammonium sulfate particles, is shown here to illustrate the lower detection efficiency effect, as shown in Fig. 4. The low detection efficiency of small particles most likely results from their reduced light scattering intensity.

2.4. Effect of laser heating on ammonium nitrate particles

Compared to the SMPS, the UHSAS tends to undersize ammonium nitrate particles. Ammonium nitrate is readily volatilized; so temperature increases might cause particle size decreases. This could occur if a small fraction of the relatively high power incident laser beam used in the UHSAS were to be absorbed. To assess this possibility, the

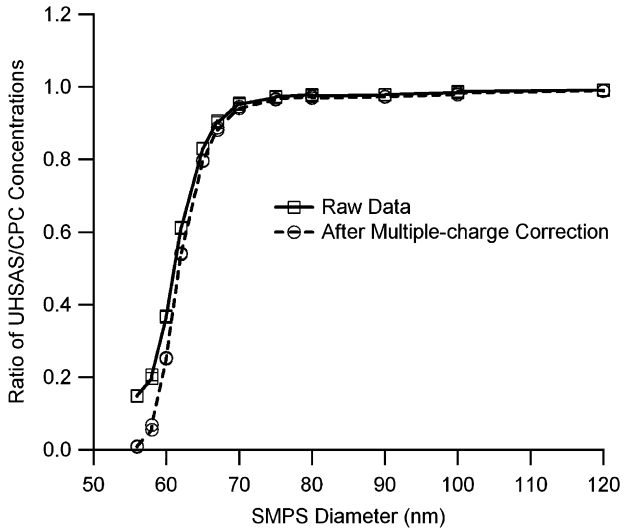

Fig. 4. Variation of ratio of the UHSAS to CPC concentrations for ammonium sulfate particles between 55 and 120 nm diameter. The ratio drops to ∼ 50% at approximately 62 nm.

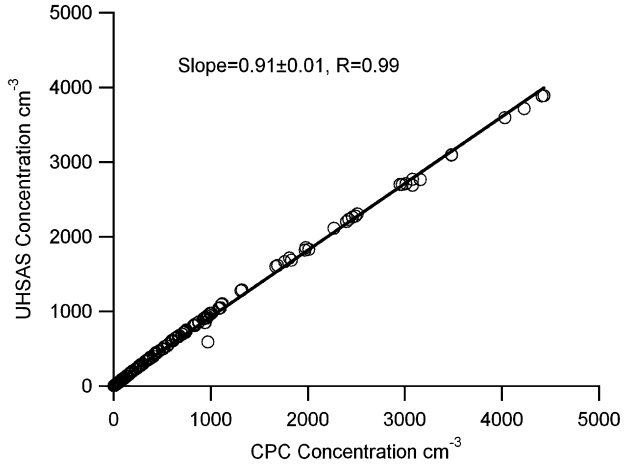

Fig. 5. Comparison of the UHSAS and CPC concentrations for PSL, ammonium nitrate, ammonium sulfate, sodium chloride particles, and PSL aggregates.

magnitude of particle heating for ammonium nitrate by the ∼ 1.0 kW, 1.054 μm laser was calculated. The decrease in particle radius with time (t) as a result of evaporation is described by Eq. (1) (Harrison, Sturges, Kitto, & Li, 1990):

$$a^2 = a_0^2 - \frac{2DMP(T)}{\rho RT}(t - t_0). \tag{1}$$

Here a_0 and a are the particle radius at the initial time, t_0, and later time, t. M is molar mass, ρ is particle density, and T is particle temperature. The diffusion coefficient, D, is 1.92×10^{-5} m^2/s for ammonium nitrate particles (Harrison et al., 1990). $P(T) = 2(K_p)^{1/2}$ is the vapor pressure. The dissociation equilibrium constant K_p is determined by (Mozurkewich, 1993)

$$\ln(K_p) = 118.87 - \frac{24084}{T} - 6.025 \ln(T). \tag{2}$$

Table 3
Measured SMPS and UHSAS diameters for ammonium nitrate particles

SMPS diameter (nm)	UHSAS diameter (nm)	Temperature increase (ΔT)	
		Calculated (K)	Required (K)
98	92	0.003	126.5
195	187	0.013	144.8
300	279	0.037	171.7
390	365	0.067	181.0
496	448	0.146	201.9
594	533	0.292	504.6

Calculated particle temperature increases due to laser heating, and temperature increases required to explain the size reduction between the SMPS and UHSAS.

The variation of particle temperature is a dynamic process based on mass and energy conservation for volatile species. For the specified conditions, non-volatile materials will attain a maximum temperature. An approximate expression for the temperature increase of non-volatile spherical particles above the ambient air temperature resulting from radiant energy absorption, is given by Chan (1975) as

$$\Delta T = I Q_{\mathrm{abs}} a / 4 k_{\mathrm{a}}, \tag{3}$$

where $k_{\mathrm{a}} = 0.026\,\mathrm{W/m\,K}$ is the thermal conductivity of ambient air at room temperature, and Q_{abs} is the particle absorption efficiency, calculated by Mie theory. The refractive index of ammonium nitrate is estimated as $1.57\text{–}2 \times 10^{-6} i$ (Gosse, Wang, Labrie, & Chylek, 1997; Jarzembski, Norman, Fuller, Srivastava, & Cutten, 2003). The laser power of the UHSAS is 1.0 kW with a beam width of 0.5 mm, corresponding to a laser intensity of about $5.1 \times 10^5\,\mathrm{W/cm^2}$. For an ambient pressure of 780 hPa, typical for our laboratory, and an ambient temperature of 20 °C, the total volumetric flow rate of the UHSAS is $975\,\mathrm{cm^3/min}$ ($910\,\mathrm{cm^3/min}$ sheath flow and $65\,\mathrm{cm^3/min}$ sample flow). The inlet nozzle (diameter 0.760 mm) produces a laminar flow velocity of $\sim 40\,\mathrm{m/s}$ for this volume flow rate, leading to a particle interaction time with the laser beam of $\sim 10\,\mu\mathrm{s}$. The laser-heating induced particle temperature increases, calculated using Eq. (3), are listed in Table 3 for ammonium nitrate particles of different diameters. They are all less than 0.3 K, so that evaporative losses are negligible. Table 3 also shows simultaneously measured SMPS and UHSAS diameters for laboratory generated ammonium nitrate particles. The UHSAS measured diameters are all smaller that those measured by the SMPS. If the low UHSAS sizes result from partial evaporation of the particles, then the heating induced temperature increases must be substantial. The corresponding required particle temperature increases, also listed in Table 3, are very much larger than those that can be attained, even if the imaginary part of the complex refractive index were to be significantly underestimated. Thus the UHSAS undersizing of ammonium nitrate particles cannot be attributed to radiant energy absorption from the laser beam in the instrument.

3. Measurements at Elk Mountain observatory

3.1. Location and sampling conditions

Elk Mountain (N41°38′, W106°32′), located in south-central Wyoming, is an isolated outlier peak of the Medicine Bow mountains in the northern front range of the Rocky Mountains. The observatory, near the summit, is at an elevation of 3320 mmsl. Population density in the local area (Carbon County) is $0.765\,\mathrm{km^{-2}}$, with the two nearest (~ 25 km) communities having populations < 1750. The closest large urban areas are Denver (246 km SW) and Salt Lake City (470 km W). The Interstate-80 highway passes 10 km north of Elk Mountain, but at approximately the same elevation as the local communities (~ 2100 mmsl).

Measurements were carried out during summer 2006. On most days ambient RH was between 10% and 40%, but rose significantly during occasional showery periods. Ambient temperature ranged from 2 to 23 °C. Aerosols were sampled through a 7.3 cm diameter vertical inlet extending 10 m above the surface. Both metal and conductive tubing were used to reduce diffusional losses of small particles. The inlet system was warmed as necessary to lower sample RH to below 25%. The size distributions of the dried aerosols were obtained using (i) a DMA (TSI, Model 3081) coupled

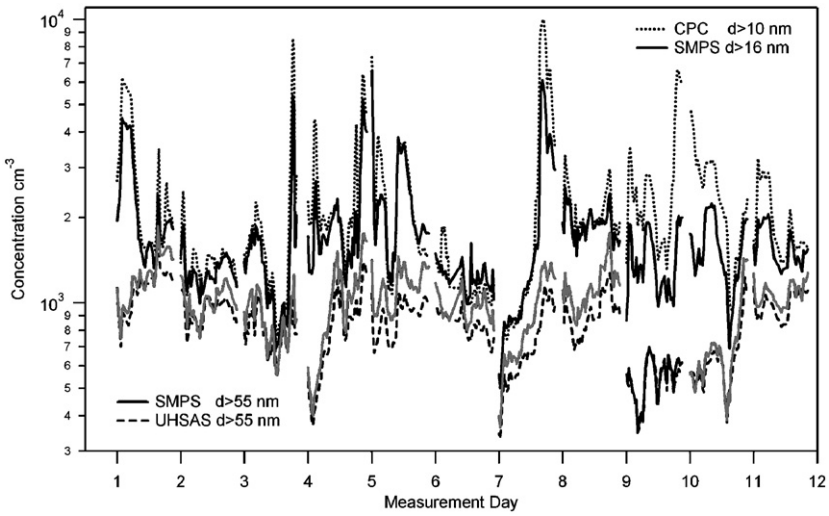

Fig. 6. Ambient aerosol concentrations measured by the CPC, SMPS, and UHSAS at Elk Mountain. The abscissa represents the eleven measurement days (July 30, 2006–August 06, 2006 and September 04–06, 2006).

to a CPC (TSI, Model 3010) to measure particle concentration as a function of mobility diameter over the size range 16–800 nm, (ii) an UHSAS to measure particle concentration as a function of optical diameter from 55 to 800 nm, and (iii) a PCASP (PMS Inc., Boulder, CO) to measure particle concentration as a function of optical diameter from 108 to 3151 nm.

3.2. Concentration measurements

Fig. 6 shows time series plots of 30 min average aerosol concentrations measured by the CPC, SMPS, and UHSAS, for 11 days (July 30–August 06, and September 04–06, 2006, UTC). Data gaps result from instrument down-time used for calibration and data archiving activities. In general, the observed concentration values are typical for unpolluted rural areas in the western USA, and are similar to those measured near the surface in remote areas of south-west Wyoming (Han, Montague, & Snider, 2003). The average total particle concentrations measured by the CPC and SMPS were $2200 \pm 1500\,\mathrm{cm}^{-3}$ and $1700 \pm 860\,\mathrm{cm}^{-3}$, but occasionally concentration values were up to three times larger than the average for a few hours. The average values are much lower than the concentrations in urban area such as Pittsburgh ($16,470\,\mathrm{cm}^{-3}$; Stanier, Khlystov, & Pandis, 2004). The UHSAS measured concentrations, illustrated in Fig. 6, varied between 300 and $1500\,\mathrm{cm}^{-3}$ with an average of $840 \pm 230\,\mathrm{cm}^{-3}$. They were lower than the CPC and SMPS concentrations presumably because of the larger lower size limit detected by the UHSAS. The occasional short-period high particle concentration episodes only observed by the CPC and SMPS must be due to increases in the concentration of small particles with diameters below the detection threshold of the UHSAS ($\sim$ 55 nm). As illustrated in Fig. 6, there is a strong positive correlation between the concentrations measured by these instruments, especially between the UHSAS and SMPS concentrations for particles larger than 55 nm. The direct concentration comparison indicates that the UHSAS, detects 86% of the ambient particles detected by the SMPS in the size range from 55 to 800 nm, and detects 93% of the ambient particles detected by the PCASP from 108 to 800 nm. The lower UHSAS concentration can be partially accounted for by the decreased detection efficiency of this instrument for particles smaller than 100 nm. The data used here for concentration comparison have not been corrected for variations in particle refractive index or non-sphericity.

3.3. Variation of aerosol size distribution

In most of the Elk Mountain observations, small particles dominate and the measured particle number size distributions peak at less than 200 nm. Particle number size distributions were observed to change considerably over a

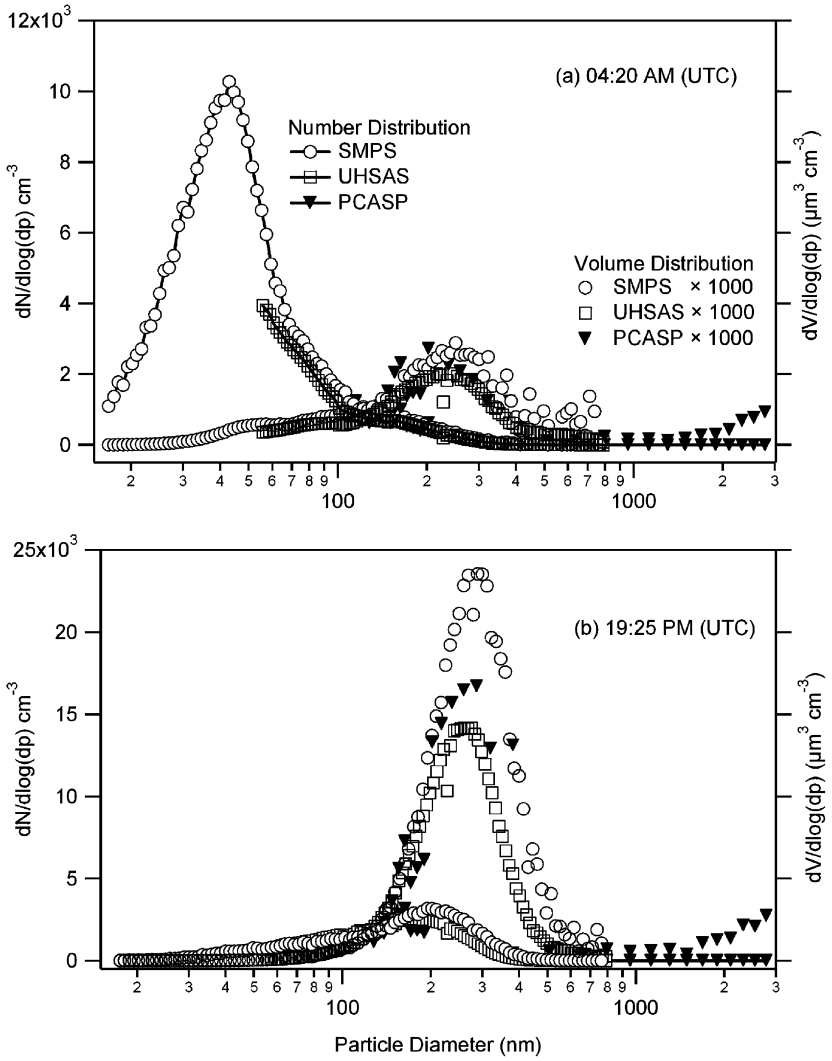

Fig. 7. Variations of aerosol size distributions, measured by the UHSAS (55–800 nm), PCASP (108–3151 nm), and SMPS (16–800 nm), at ELK Mountain on July 30, 2006 (UTC).

few hours, often with the appearance of multiple modes. Fig. 7 shows representative examples of 30 min average size distributions measured at Elk Mountain on July 30, 2006 (UTC). These distributions are uncorrected for variations in refractive index and particle non-sphericity. For aerosol number distributions, the principal size mode measured by the SMPS increased from $\sim$ 40 to $\sim$ 200 nm during the course of the day. At about 4:20 am UTC (22:20 pm, mdt), small particles dominated and the principal mode size measured by the SMPS peaked at $\sim$ 40 nm, which is below the lower size detection limit of the UHSAS. A smoothly decreasing size distribution without a corresponding peak was observed by the UHSAS, as shown in Fig. 7(a). Undercounting of total particle number density by the UHSAS is apparent at small diameters. By about 19:25 pm UTC (13:25 pm, mdt), as shown in Fig. 7(b), the principle size mode switched to $\sim$ 200 nm. The UHSAS measurements show a similar developing profile of size distributions as the SMPS, but with slightly smaller peak sizes. Concentrations of large particles ($>$ 1 μm), measured by the PCASP, were low. It was evident that the PCASP number size distributions were consistent with the measurements from the UHSAS and SMPS in the overlapping size ranges. For the particle volume distributions shown in Fig. 7, the mode sizes do not vary significantly and are consistent with each other. The variability with time of the particle number size distributions measured by the SMPS (every 5 min) and the UHSAS (every 1 min) is illustrated in greater detail by the image plots

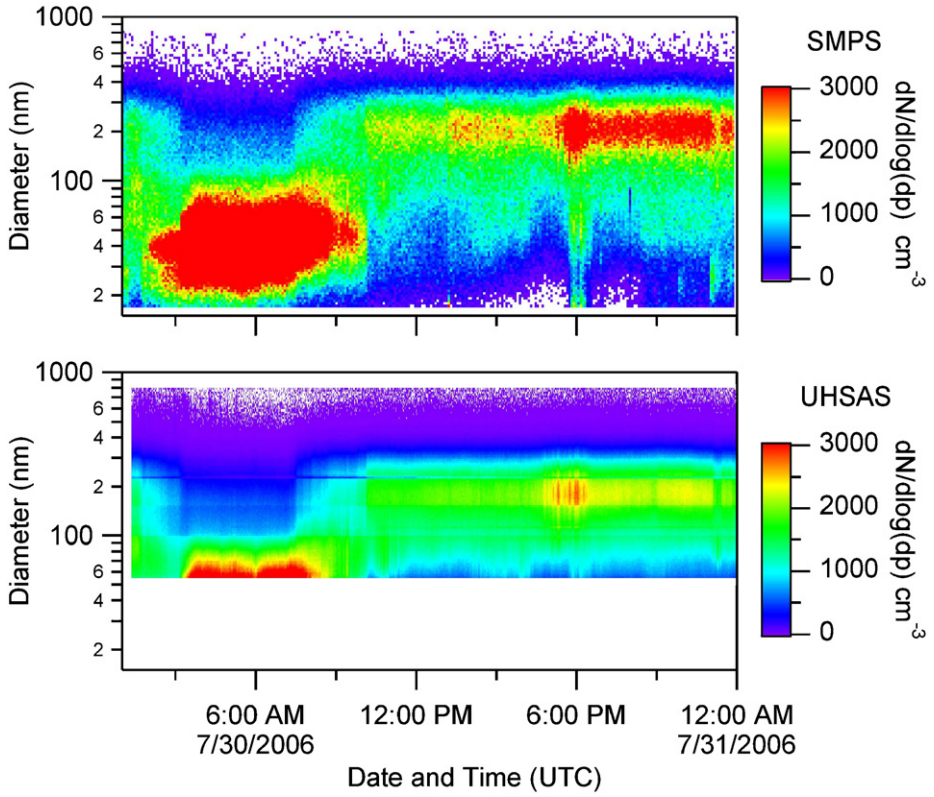

Fig. 8. Image plots of the time dependence of particle number size distribution measured at Elk Mountain observatory by the SMPS (upper panel) and UHSAS (lower panel) on July 30, 2006 (UTC).

shown in Fig. 8. They show that the shift in mode size does not occur gradually throughout the day, but takes place quite rapidly before sunrise, between 09:00 and 11:00 (UTC). Indeed, before and after this period, the prevailing mode size remains relatively constant. The plots visually confirm both the relatively smaller modal peak size and mode diameter measured by the UHSAS later in the day and the inability of the UHSAS to detect a large fraction of the very small particles that are present before 09:00.

Significant variation of the observed particle size distributions at Elk Mountain is to be expected, because many factors, including parcel advection, convective mixing promoted by daytime upslope flow, insolation variations affecting air chemistry, local cloud extent, and changes in regional source strengths, such as forest fire outbreaks, can affect particle concentrations and aging processes. In addition, we are aware that the UHSAS measured particle sizes always tend to be smaller than those determined by the SMPS, as a result of particle non-sphericity and deviations in particle refractive index from the value used for the UHSAS calibration. An assessment of these factors requires a detailed examination of the chemical and physical properties of the Elk Mountain aerosols. That analysis is beyond the scope of this paper and will be reported elsewhere.

4. Conclusions

The UHSAS detects and sizes particles with diameters > 55 nm with high accuracy and good size resolution. For ammonium sulfate particles, the lower detection size limit, defined as the size corresponding to a detection efficiency of 50%, is 62 ± 2 nm. Below this threshold diameter, detection efficiencies rapidly decrease. In general, the UHSAS measured diameters are slightly smaller than those measured by the SMPS, depending on particle type. Shape factors of sodium chloride particles and PSL doublets have no significant influence on the UHSAS size measurement. UHSAS and CPC measured concentrations are in good agreement when particle diameters are larger than 100 nm and number

densities are below 3000 cm^{-3}, when coincidence counting losses are negligible. For particles smaller than 100 nm, the UHSAS has a significant concentration measurement error due to the low scattered light intensity from small particles. The UHSAS has been field tested at a remote mid-continental high altitude site in Wyoming. The UHSAS measured particle number concentrations average $840 \pm 230\,cm^{-3}$, whereas those from a condensation particle counter (CPC) average $2200 \pm 1500\,cm^{-3}$. The highest number densities were monitored by the CPC during periods when most particle diameters were less than 55 nm. In concentration comparisons of the same size ranges, the UHSAS detected 86% of the ambient particles detected by the SMPS, and 93% of the ambient particles detected by the PCASP. Differences in the size detection ranges of the instruments, particle non-sphericity and refractive index variability can account for the differences between the observed size distributions.

Acknowledgments

This work was supported by the National Science Foundation under Grant 0441836 and the W.M. Keck Foundation. The significant effort of the department's technical staff in preparing instrumentation for the Laramie measurements and in deploying instrumentation to Elk Mountain is gratefully acknowledged. We also thank the reviewers and editor for their helpful comments.

References

Ames, R. B., Hand, J. L., Kreidenweis, S. M., Day, D. E., & Malm, W. C. (2000). Optical measurements of aerosol size distributions in Great Smoky Mountains National Park: Dry aerosol characterization. *Journal of the Air and Waste Management Association*, *50*, 665–676.

Barnard, J. C., & Harrison, L. C. (1988). Monotonic responses from monochromatic optical particle counters. *Applied Optics*, *27*, 584–592.

Chan, C. H. (1975). Effective absorption for thermal blooming due to aerosols. *Applied Physics Letters*, *26*, 628–630.

DeCarlo, P. F., Slowik, J. G., Worsnop, D. R., Davidovits, P., & Jimenez, J. L. (2004). Particle morphology and density characterization by combined mobility and aerodynamic diameter measurements. Part 1: Theory. *Aerosol Science and Technology*, *38*, 1185–1205.

Dick, W. D., Ziemann, P. J., Huang, P. F., & McMurry, P. H. (1998). Optical shape fraction measurements of submicrometer laboratory and atmospheric aerosols. *Measurement Science and Technology*, *9*, 183–196.

Gosse, S. F., Wang, M. Y., Labrie, D., & Chylek, P. (1997). Imaginary part of the refractive index of sulfates and nitrates in the 0.7–2.6 μm spectral region. *Applied Optics*, *36*, 3622–3634.

Han, Z. G., Montague, D. C., & Snider, J. R. (2003). Airborne measurements of aerosol extinction in the lower and middle troposphere over Wyoming, USA. *Atmospheric Environment*, *37*, 789–802.

Hand, J. L., Kreidenweis, S. M., Kreisberg, N., Hering, S., Stolzenburg, M., Dick, W., & McMurry, P. H. (2002). Comparisons of aerosol properties measured by impactors and light scattering from individual particles: Refractive index, number and volume concentrations, and size distributions. *Atmospheric Environment*, *36*, 1853–1861.

Harrison, R. M., Sturges, W. T., Kitto, A. M. N., & Li, Y. Q. (1990). Kinetics of evaporation of ammonium chloride and ammonium nitrate aerosols. *Atmospheric Environment*, *24A*(7), 1883–1888.

Jarzembski, M. A., Norman, M. L., Fuller, K. A., Srivastava, V., & Cutten, D. R. (2003). Complex refractive index of ammonium nitrate in the 2–20 μm spectral range. *Applied Optics*, *42*, 922–930.

Lightstone, J. M., Onasch, T. B., Imre, D., & Oatis, S. (2000). Deliquescence, efflorescence, and water activity in ammonium nitrate and mixed ammonium nitrate/succinic acid microparticles. *Journal of Physical Chemistry A*, *104*, 9337–9346.

Liu, P. S. K., Leaitch, W. R. J., Strapp, W., & Wasey, M. A. (1992). Response of particle measuring systems airborne ASASP and PCASP to NaCl and latex particles. *Aerosol Science and Technology*, *16*, 83–95.

McMurry, P. H. (2000). A review of atmospheric aerosol measurements. *Atmospheric Environment*, *34*, 1959–1999.

Mozurkewich, M. (1993). The dissociation constant of ammonium nitrate and its dependence of temperature, relative humidity and particle size. *Atmospheric Environment*, *27A*(2), 261–270.

Perry, R. J., Hunt, A. J., & Huffman, D. R. (1978). Experimental determinations of Mueller scattering matrices for nonspherical particles. *Applied Optics*, *17*, 2700–2706.

Pinnick, R. G., & Rosen, J. M. (1979). Response of Knollenberg light-scattering counters to non-spherical doublet polystyrene latex aerosols. *Journal of Aerosol Science*, *10*, 533–538.

Quinten, M., Friehmelt, R., & Ebert, K. F. (2000). Sizing of aggregates of spheres by a white-light optical counter with 90 scattering angle. *Journal of Aerosol Science*, *32*, 63–72.

Stanier, C. O., Khlystov, A. Y., & Pandis, S. N. (2004). Ambient aerosol size distributions and number concentrations measured during the Pittsburgh air quality study (PAQS). *Atmospheric Environment*, *38*, 3275–3284.

Tang, I. N., & Munkelwitz, H. R. (1994). Water activities, densities, and refractive indexes of aqueous sulfates and sodium nitrate droplets of atmospheric importance. *Journal of Geophysical Research—Atmospheres*, *99*(D9), 18801–18808.

Weschler, C. J., & Shields, H. C. (2003). Experiments probing the influence of air exchange rates on secondary organic aerosols derived from indoor chemistry. *Atmospheric Environment*, *37*, 5621–5631.

Zelenyuk, A., Cai, Y., Chieffo, L., & Imre, D. (2005). High precision density measurements of single particles: the density of metastable phases. *Aerosol Science and Technology*, *39*, 972–986.